J. Min. Metall. Sect. B-Metall. 49 (3) B (2013) 237 - 244

Journal of Mining and Metallurgy, Section B: Metallurgy

INTRAGRANULAR FERRITE MORPHOLOGIES IN MEDIUM CARBON VANADIUM-MICROALLOYED STEEL

A. Fadel [a], D. Glišić [a], N. Radović [a, #], D. Drobnjak [a]

[a] University of Belgrade, Faculty of Technology and Metallurgy, Department of Metallurgical Engineering, Belgrade, Serbia

(Received 20 August 2012; accepted 03 December 2012)

Abstract

The aim of this work was to determine TTT diagram of medium carbon V-N micro-alloyed steel with emphasis on the development of intragranular ferrite morphologies. The isothermal treatment was carried out at 350, 400, 450, 500, 550 and 600 °C. These treatments were interrupted at different times in order to analyze the evolution of the microstructure. Metallographic evaluation was done using optical and scanning electron microscopy (SEM). The results show that at high temperatures (≥ 500 °C) polygonal intragranulary nucleated ferrite idiomorphs, combined with grain boundary ferrite and pearlite were produced and followed by an incomplete transformation phenomenon. At intermediate temperatures (450, 500 °C) an interloced acicular ferrite (AF) microstructure is produced, and at low temperatures (400, 350 °C) the sheave of parallel acicular ferrite plates, similar to bainitic sheaves but intragranularly nucleated were observed. In addition to sheaf type acicular ferrite, the grain boundary nucleated bainitic sheaves are observed.

Keywords: TTT diagram; Acicular Ferrite; Bainite; Grain Boundary Ferrite; Widmanstatten and Polygonal Ferrite; Pearlite.

1. Introduction

The markets such as automotive components demand increased combination of strength and impact toughness, together with and reduction of weight and costs. The high strength forging steels have traditonally developed their strength and toughness by quenching and tempering following hot forging. This multi-stage process extends production time and can cause distortion in complex shaped components, so its increases in production cost. In order to overcome the previous proplem the microalloyed forging steels [1,2] have been developed: they achieve their strength during air cooling after forging thus removing the need for secondary heat treatment. By contrast the air cooled structure is generally composed of coarse ferrite and pearlite and this can limit impact toughness. Therefore there is a strong need to refine microstruture. Thereby several studies on microalloyed forging steels have concentrated on determining the microstructural features that control toughness [3-7]. The acicular ferrite has also been developed in a medium carbon forging steels [3,5,8-11] or a low carbon steel [12]. Good combination of mechanical properties of medium carbon V-N microalloyed steels are attributed to the dominant presence of fine ferrite-pearlite and acicular ferrite microstructure, while the presence of bainitic sheaves leads to decrase in toughness [13]. Acicular ferrite and bainite are usually considered to be formed by the same transformation mechanism [14-17]. The acicular ferrite formation is a mechanism competitive with bainite formation. Acicular ferrite, as bainite, is formed by a shear-diffusional mechanism. The main difference between acicular ferrite and bainite is related to the nucleation sites. The acicular ferrite is in fact intragranularly nucleate bainite [9,14, 16-21]. Both microstructures develop in the same range of temperature: below the high temperatures where ferrite and pearlite form, but above the martensite start temperature. The bainite initiates at the austenite grain boundaries, forming sheaves of parallel plates with the same crystallographic orientation, where acicular ferrite is nucleated intragranulary at nonmetallic inclusions [14,16, 21-23]. There are several mechanisms proposed to explain why non-metallic inclusions favour the nucleation of ferrite : (i) the existence of local variations of the chemistry of the matrix. (ii) generation of strain-stress field around the inclusions due to the different thermal expansion coefficient of austenite and inclusion. (iii) improvement in the global energetic balance of the

* *Corresponding author: nenrad@tmf.bg.ac.rs*

DOI:10.2298/JMMB120820001F

transformation by the reduction of the austenite-inclusion surface. (iv) the creation of low-energy surfaces between ferrite and inclusion with the existence of a good lattice matching between them [10]. The microstructure of acicular ferrite is less organized when compared with the ordinary bainite, the acicular ferrite have chaotic arrangement of interlocked plates. This microstructure is better suited to deflect propagation cleavage cracks and therefore more desirable from toughness point of view in comparison to Bainite Sheaves [13, 17, 24]. In some recent studies, an improved toughness, observed in medium-carbon steels is associated with AF [13, 22-25].

The purpose of the present study is to clarify experimentally the TTT diagram of V-N –Steel. Moreover the influence of isothermal transformation temperature and time on the nucleation of intragranular ferrite and indirectly, on the development of the intra-granular acicular ferrite in microalloyed steel has been investigated.

2. Experimental Procedure

The chemical composition of steel studied in the present work is given in Table 1. The steel used for this investigation was made by full-scale casting and fabricated into 19mm diameter bar by full-scale forging and hot-rolling. Representative hot-rolled steel bars were homogenized at 1250 °C for 4 hours, in the presence of argon as protective atmosphere, to minimize any effect of chemical segregation. After annealing, the samples were water quenched, and then the specimens with 12mm length were cut from 19 diameter bars and austenitized at 1100 °C for 10 min in an argon atmosphere. After austenitization, specimens were isothermally transformed at different temperatures ranging from 350 °C to 600 °C at different times between 2 and 1200 s. Finally, specimens were water quenched to room temperature. The samples were cut, mechanically ground and then polished to 1μm diamond finish paste using standardized metallographic techniques and subsequently etched in 2 % nital for their observation by optical and scanning electron microscopy (SEM). The samples were used to reveal grain boundaries by thermal etching based on the combination of heat treatment and thermal etching (TE) method [26, 27]. The prior austenite grain size generated by austenitizing at 1100 °C for 10 min was determined using a linear intercept technique and found to be 57 ±3μm.

3. Results and Discussion

The equilibrium temperatures for complete dissolution of VN in present steel was calculated according to the equation given in Ref. [28], and it was estimated to be 1100 °C. The measured austenite grain size at this temperature is 57 ±3μm, and is expected to enhance intragranular AF formation rather than bainite by increasing the ratio between intragranular and grain boundary sites [29, 30]

The experimentally determined TTT diagram is presented in Figure 1. The Grain Boundary Ferrite (GBF) the first phase to nucleate over the entire temperature range tested, is shown in Figures 2(a-e) and is represented by a two C curves, describing the effects of diffusional (upper C curve) and displacive (lower C curve) transformations. Within the lower C-curve a clear indication of Widmanstatten nucleation is observed Figure 2(f,g). At a later stage the different intra-granular ferrite (IGF) morphologies are initiated, what is represented again by the two- C (IGF) nucleation curves in Figure 1. In the (IGF) region, three different morphologies have been observed depending upon the isothermal treatment temperature.

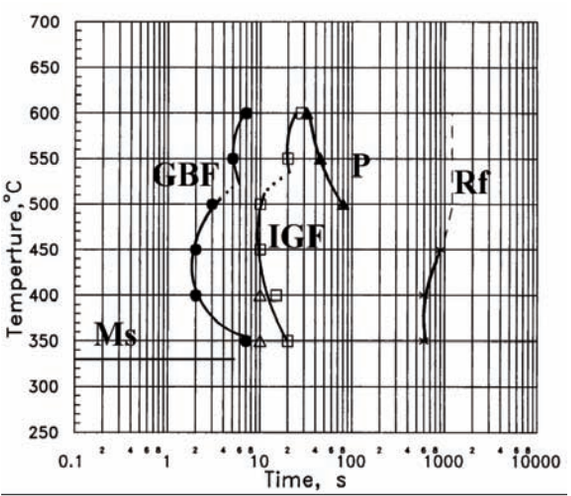

Figure 1. *Time - Temperature - Transformation (TTT) diagram of present steel showing the Grain Boundary Ferrite (GBF) start curve, Intra-Granular Ferrite (IGF) start curve, Bainite Sheaves (BS) are indicated by open triangles, Pearlite (P) start curve and Reaction Finish (RF) Curve (where incomplete reaction is indicated by dashed line).*

Firstly, at high temperatures (≥ 550 °C) intragranulary nucleated ferrite combined with grain boundary ferrite (GBF) and pearlite (P) are produced,

Table 1. *Chemical composition of the experimental steel (wt%)*

C	Si	Mn	P	S	Cr	Ni	Cu	Al	Mo	Ti	V	N
0.256	0.416	1.451	0.0113	0.0112	0.201	0.149	0.183	0.038	0.023	0.002	0.99	0.0235

Figure 3(a,b). The intragranular ferrite is characterized by polygonal idiomorphic (IGF) Ferrite. The idiomorphic ferrite nucleates intra-granularly at the inclusions distributed inside the austenite grains, and the volume fraction of idiomorphic ferrite is related to the volume fraction of inclusions in steel [31]. The transformation after1200s of isothermal treatment at 550 and 600 °C reveals that a fraction of austenite remains untransformed, Fig. 4(a,b). This phenomenon has been described by Bhadeshia [16, 32-34] and is known as incomplete reaction phenomenon. It is presented by dashed line on TTT diagram in Figure 1. At 600 °C, there was thicker grain boundary ferrite than at 550 °C , but in respect to the population density of ferrite plates inside the prior austenite grains it is lower as can be seen in Fig.3(a,b). This seems to indicate that at 600 °C, the carbon rejected from the ferrite plates diffuses rapidly leading to supersaturation in austenite. The carbon enrichement of the remaining austenite together with relatively small driving force for transformation at 600 °C is enough to inhibit the formation of new ferrite plates [32].

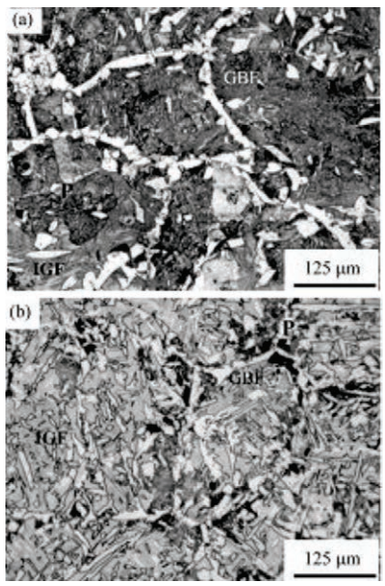

Figure 3. *(a,b).Optical micrographs showing the microstructures and population density obtained after120s of isothermal treatment at high temperature (a) 600 °C, (b) 550 °C*

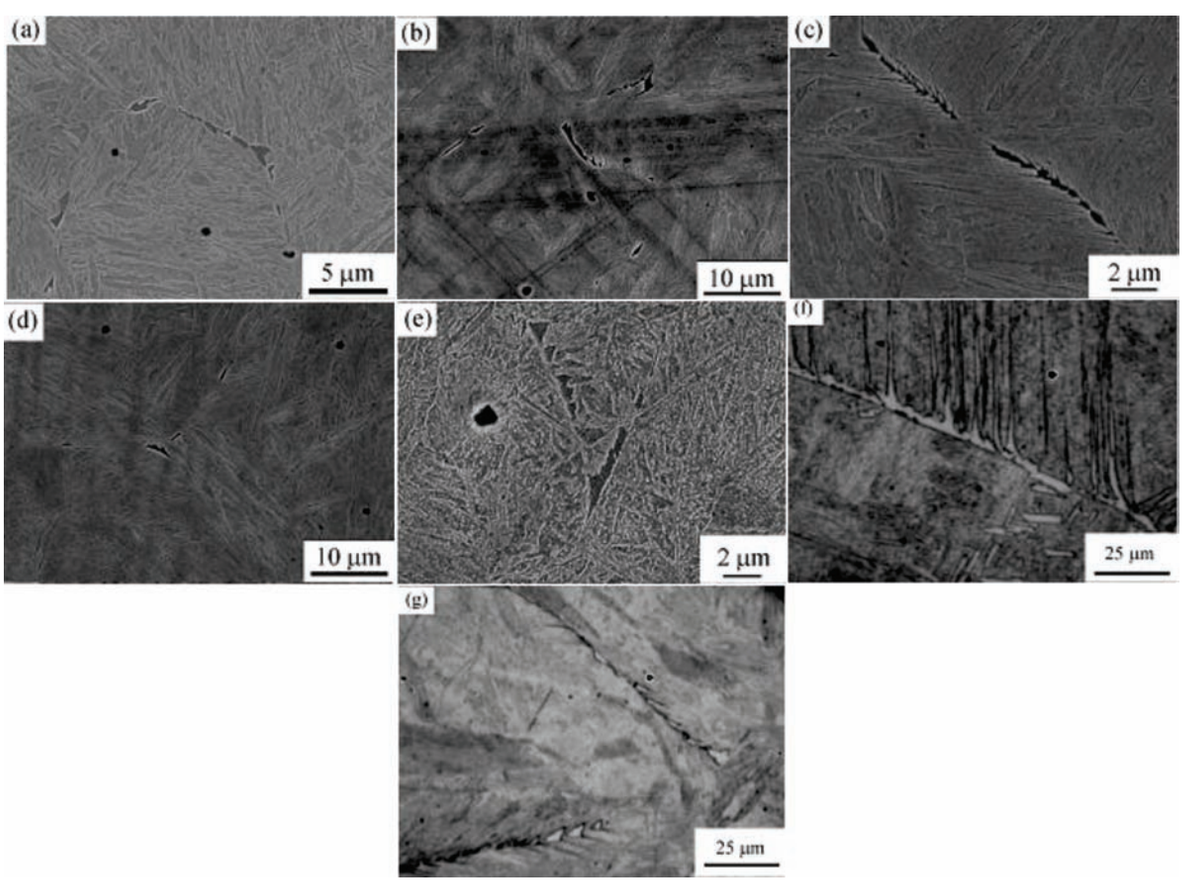

Figure 2. *(a-g). SEM images and optical micrographs showing onset of Grain Boundary Ferrite (GBF)/ Widmanstatten formation at different isothermal treatment temperatures. Thus, for (a) 10s at 600°C.(b) 5s at 550°C. (c) 3s at 500°C (d) 2s at 450°C (e) 2s at 400°C. (f) 10s at 400°C. (g) 2s at 450°C.*

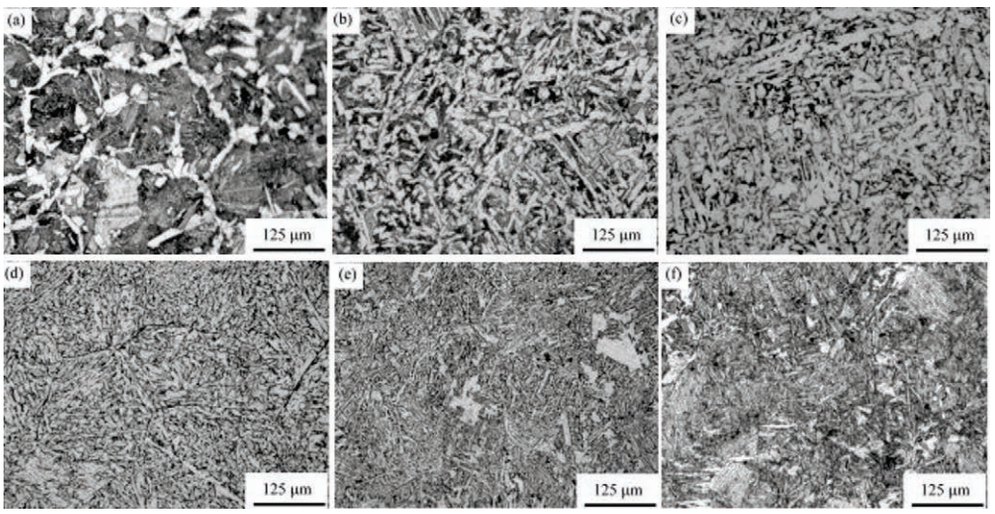

Figure 4. *(a-f).Optical micrographs showing the microstructures obtained after 1200s at low (350, 400 °C), intermediate (450, 500 °C) and high (550, 600 °C) of isothermal transformation temperatures. Thus, for (a) 600 °C (b) 550 °C (c) 500 °C (d) 450 °C (e) 400 °C (f) 350 °C.*

Second type of intragranular ferrite morphologies occur at intermediate temperature (450 and 500 °C). An interlocked acicular ferrite(AF) microstructure is produced as can be seen in Fig.5(d). At the initial stages, the nucleation of the primary ferrite plates takes place intragranularly at second phase particles (nonmetallic inclusions) present in the austenite, as can be seen in Figure 5 (a,b), which is in good agreement with [14, 16, 17, 24, 31, 32]. The micrograph present in Figure 5(c) and an energy dispersive X-ray (EDX) spectrum analysis illustrate a typical active inclusion, with the corresponding chemical analysis at different points of the particle, it is identified as Ca-treated manganese sulfides inclusion core covered or at least partially covered with VN or V(C, N) complex precipitate. This is in good agreement with results reported by Ochi et al and Ishikawa et al. [34, 35]. The manganese sulfides have been reported previously to be active on nucleating acicular ferrite [8, 10, 23, 24, 31, 34, 36]. Moreover the inclusion size and shape is modified by Ca treatment (Morphology altered by Ca addition - in order to control and modify the shape of MnS inclusions, i.e. to get spherical shape and very low deformability). The majority of MnS inclusions in the Ca-treated steels were globular (Ca,Mn)S particles. MnS particles represented the largest contribution (60-70%) to the overall inclusion volume fraction [37]. However the nucleation of AF plates is not restricted to inclusions, new ferrite plates can grow from pre-existing ones, as can be observed in Figure 6 (b), which supports the view, that nucleation occurs sympathetically.

In Figure 6(b), the sympathetic nucleation of secondary acicular ferrite plates has been observed to occur at the austenite/primary acicular ferrite interface and continue to grow within the austenite matrix until impingement occurs with other plates. An example of impingement processes is illustrated in the SEM micrographs as clearly shown in Figure 6(c). The result

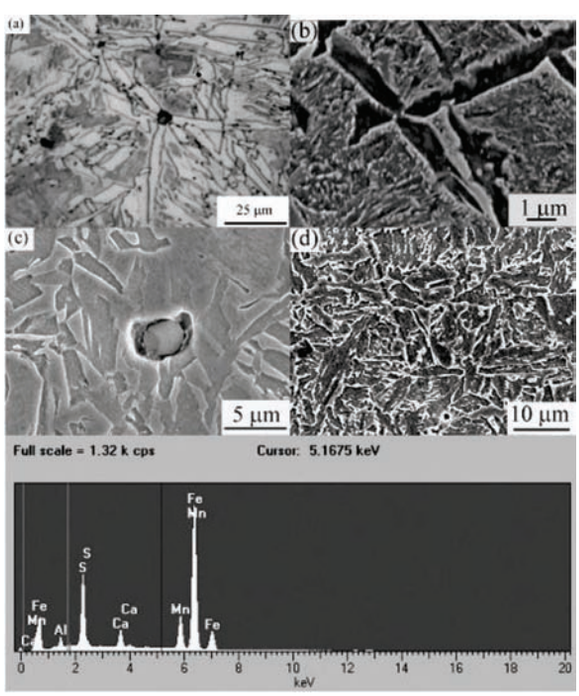

Figure 5. (a,b) Optical micrographs and SEM image showing onset of acicular ferrite on inclusion after (a) 30s at 500°C. (b) 20s at 450 °C. (c) SEM image and EDX spectrum showing the type of the inclusion exist. 5(d) SEM image showing the acicular ferrite microstructure after 1200s at 450 °C.

of multiple sympathetic nucleation is an interlocking ferrite network, and after sufficient time, it results into a complex interlocking ferrite microstructure, characteristic of acicular ferrite, such as that shown in Fig. 5(d). The resulting microstructure with fully acicular ferrite structure in medium carbon microalloyed steel, with the exception of a few small bainitic zones is in good agreement with published data [8]. The present results clearly show no carbides were observed to form within the ferrite plates at intermediate time and temperature (450-500 °C) as can be seen in Fig. 6(e). This is good a greement with published data [16, 23, 32]. The incubation time is the shortest time at which it was possible to find grain boundary ferrite, and it is found to be approximately at 450°C (Figure 1). The maximum acicular ferrite content in the present steel is found for treatment carried out at 450°C. This treatment is characterised by the fully acicular ferrite formation. On the other hand, it is possible to find, in certain localized places, bainite formed at the grain boundaries, as shown in Figure 6(d). At 450-500 °C, the majority of plates are free of precipitates due to the carbon diffusion is high, favouring the decarburisation of the majority of ferrite plates, as can be seen in Fig. 6(e) and 5(c). The microstructure can be identified as upper acicular ferrite. The onset of pearlite at different a treatment temperature (≥ 500 °C) is illustrated in Figure 7 (a-d) and P-line in Figure 1. Also it is apparent, from the shape of TTT-diagram in Figure 1, that the bainitic transformation start temperature (B_S) occurs at 530 ± 10 °C . This result is in good agreement with B_S temperature calculated by different empirical formulas [16, 38-41].

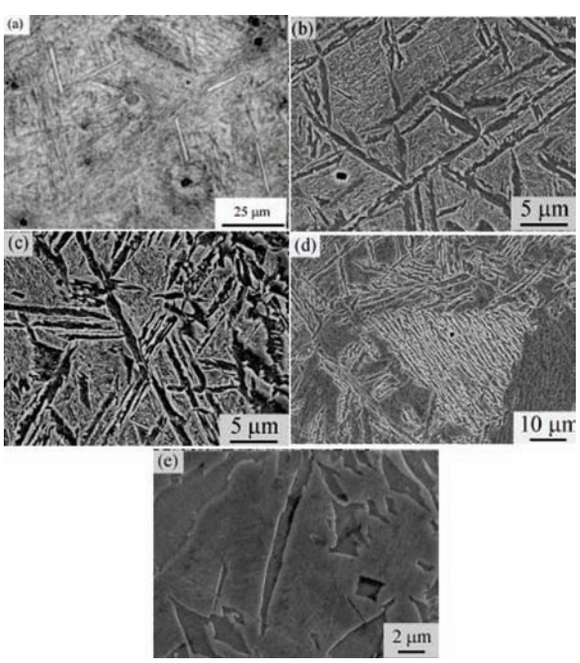

Figure 6. *(a) Optical micrograph image after10s at 450 °C; (b, c) SEM image after 20s at 450 °C (d) SEM image showing an isolated bainite area formed in the steel sample treated for 30s at 450 °C; 6 (e) SEM image show the majority of plates are free of precipitates after 30s at 500 °C.*

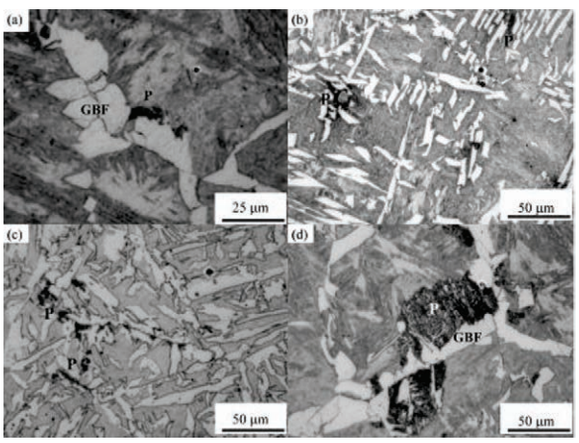

Figure 7. *(a-c) Optical micrographs showing the pearlite onset at (≥ 500 °C). (a) 30s at 600 °C. (b) 45s at 550 °C. (c) 80s at 500 °C (d) Optical micrograph showing intragranulary nucleated ferrite combined with grain boundary ferrite (GBF) and pearlite (P) at 600 °C for 60s as isothermal time.*

The third type of intragranular ferrite morphology exist at low temperatures (350, 400 °C). Two different morphologies are present at the beginning of the transformation, Bainite sheaves BS as can seen in Figure 8(a) and interlocked AF as can seen in Figure 8(b).The origin of Bainitic sheaves are exclusively the grain boundaries. The nucleation of Bainitic Sheaves is indicated in Fig. 1. by open triangles.When the isothermal treatment times is increased a new intragranular morphology known as the sheaf type acicular ferrite (STAF) [23] is observed as can be seen in Figure 8(c). There is tendency to form sheaves composed of parallel plates but the nucleation does not take place at the grain boundaries. The transition between an interlocked morphology and sheaf type morphology was estimated to occur at 450/400 °C. This morphological transition can be related to the transition from upper to lower acicular ferrite and to differences in the carbon concentration profiles in the parent austenite in the front of the interface of the primary acicular plates depending on the treatment temperature. As it is suggested [22,23], at initial stages for the transformation at 400°C, the carbon concentration in austenite close to the tips of primary plates is lower than at the faces (side direction). Therefore, instead of growth in side direction, nucleation on the tips of present sheaf is favoured, due to carbon enrichment on side direction. Overall, in final microstructure sheaf type AF dominates on the

expense of interlocked type. [22,23]. Whereas at 450 °C, the stronger diffusion of carbon from the austenite/ferrite interfaces makes possible the plate nucleation on faces i.e the carbon is able to diffuse away from the austenite / ferrite interfaces in shorter times than at 400 °C. This is expected to allow the nucleation of new ferrite variants on the primary plate faces in agreement with interlocked plate microstructure obtained at 450 °C, as seen in Figures 6(b),5(d) and 4(d).

The martensite–start (M_S) temperature in the present steel is experimentally determined. The result show that it occures close to 330 °C. This result is in good agreement with martensite–start (M_S) temperature calculated by different empirical equations [41-45].

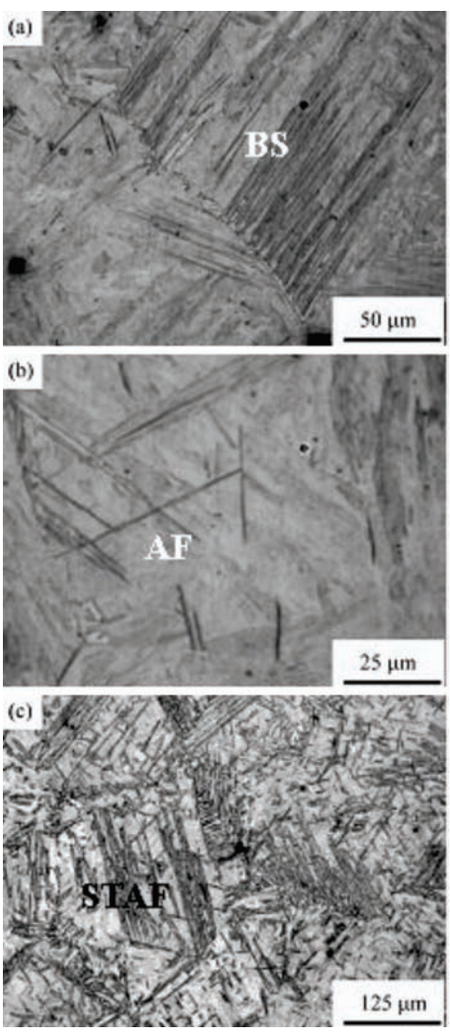

Figure 8. *(a ,b) Optical micrographs showing bainitic sheaves and acicular ferrite onset after 10s of isothermal treatment at 350 °C respectively and 8 (c).Optical micrograph showing bainitic sheaves and sheaf type acicular ferrite (STAF) formation after 20s of treatment at 350 °C.*

Microstructures in Figures 4(a-f) are obtained after 1200s of isothermal treatments at 350, 400, 450, 500, 550 and 600 °C. They refer to the competition of transformation (finish line in Fig.1.). At temperature ≥ 550 °C, the austenite has been transformed into a mixture of allotriomorphic and idiomorphic ferrite and pearlite. However, some of the austenite remains stable, and only after the final water quenching it transforms to martensite as shown in Figure 3(a,b). At 500 °C, some small colonies of pearlite have been formed between the acicular ferrite plates as shown in Figure 9(a,b). As the transformation temperature is reduced to 450 °C, the refinement of the ferrite plate is achieved (a great number of adjacent ferrite plates present) as shown in Figure 4 (d).and 5(d) In this case, the austenite has transformed to acicular ferrite, giving rise to the characteristic interlocked microstructure as seen in Fig. 5(d) . As temperature is decreased to 400 and 350 °C, mainly two morphologies are observed BS and sheaf type acicular ferrite, as demonstrated in Fig. 8(c).

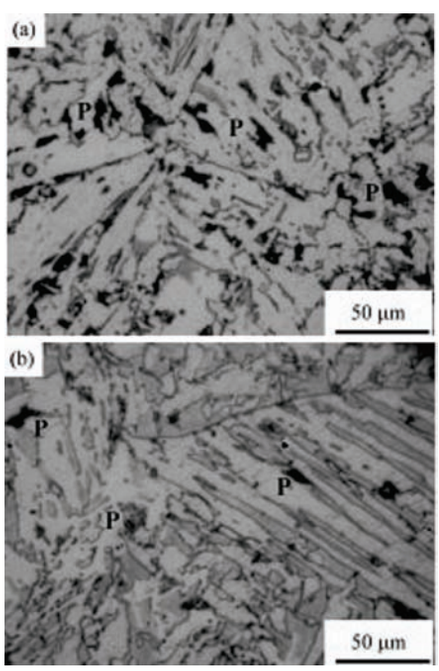

Figure 9. *(a, b) Optical micrographs showing some small colonies of pearlite formed between the acicular ferrite plates at 500°C after (a) 600s.and (b) 240s of isothermal treatment.*

4. Conclusions

Isothermal decomposition of medium carbon vanadium microalloyed austenite was evaluated by optical and SEM metallography.The four curves are found to be relevant to this of transformation.

(1) Grain boundary ferrite is the first phase to be

generated at all temepratures. In the lower temperature range the widmanstetten ferrite is formed, while on higher temperatures grain boundary allotriomorphs are produced. This difference is attributed to displacive nature of transformation at lower and diffusional transformation at higher temperatures.

(2) Second curve is related to nucleation of Intragranular ferrite (IGF). In the lower temperature range (350–400 ºC) acicular ferrite plates are grouped in sheaves; at intermediate temperatures (450–500 ºC), a more interlocked microstructure of acicular ferrite was clearly obsorved, while microstructure generated at high temperatures (550–600 ºC) is characterized by polygonal idiomorphic ferrite.

(3) Third curve is related to onset of pearlite. It occurs at temperatures ≥ 500 ºC, followed by an incomplete reaction phenomenon.

(4) The transition between an acicular ferrite sheaf morphology and interlocked microstructure is observed to take place at 400/450 ºC. However the bainitic sheaves are frequently observed when the isothermal transformation time is increased at 400 ºC and temperature diminishes to 350 °C.

(5) Finish of transformation was clearly observed at temperatures below 500°C. However at 550 and 600°C, incomplete reaction phenomenon occurs. This behaviour is attributed to carbon enrichment in austenite and decrease of driving force for austenite decomposition.

Acknowledgements

The authors are indebted to Ministry of Education and Science of Serbia for financial support (Project OI174004) and Serbian Oil Company for supplying experimental material. AF acknowledges the Ministry of Higher Education of Libya for PhD scholarship.

References

[1] G. Krauss, S.K. Banerji (Eds.), Fundamentals of Microalloying Forging Steels, The Metallurgical Society TMS,Warrendale, PA, USA,1987, p. 55.

[2] P.E. Reynolds, Heat Treat. Met. 3 (1990) 69 -72.

[3] M.A. Linaza, J.L. Romero, J.M. Rodrıguez-Ibabe, J.J. Urcola: Scripta Met. Mater. 29 (9) (1993) 1217–1222.

[4] I. Madariaga, I. Gutierrez, Materials Science Forum., 284-286 (1998) 419-426.

[5] M.A. Linaza, J.L. Romero, J.M. Rodrıguez-Ibabe, J.J. Urcola, Scripta Met. Mater., 32 (3) (1995) 395–400.

[6] A. Echeverria, J.M. Rodrıguez-Ibabe, Scripta Mater., 41 (2) (1999) 131–136.

[7] M.J. Balart, C.L. Davis, M. Strangwood, Mater. Sci. Eng., A284(2000) 1–13.

[8] I. Madariaga, J. L. Romero, and I. Gutierrez: Met. and Mat. Tran ., 29 A (1998) 1003-1015.

[9] Garcia de Andres, C., Capdevila, C., Caballero, F.G., & D San Martin. J.of Mat. Sci., 36 (2001) 565-571.

[10] I. Madariaga and I. Gutierrez: Acta mater., 47 (3) (1999) 951-960.

[11] I. Madariaga and I. Gutierrez : Scripta mater., 37 (8) (1997) 1185-1192.

[12] M. Dıaz-Fuentes, I. Madariaga, J.M. Rodrıguez-Ibabe, and I. Gutierrez: J.Construct, Steel Res., 46 (1-3) (1998) 413-14.

[13] D. Glisic, N. Radovic, A. Koprivica, A. Fadel and D. Drobnjak: ISIJ Int., 50 (4) (2010) 601–606

[14] S.S. Babu and H.K. D. H. Bhadeshia: Mat. Trans., JIM 32 (8) (1991) 679-688.

[15] M.J. Perricone: Bainitic Structures, Metallography and Microstructures, Metals Park, OH, ASM International, USA 2004, p.179.

[16] H.K.D.H.Bahdeshia: Bainite in Steels, The Institute of Materials, London, 2001, p.237.

[17] A. Khodobandeh, M. Jahazi, S. Yue and P. Bocher: ISIJ Int., 45 (2) (2005) 272-280.

[18] C. Capdevila, J. P. Ferrer, C. Garcia-Mateo, F. G. Caballero, V. Lopez and C. G. DeAndres: ISIJ Int., 46 (7) (2006) 1093-1100.

[19] C. Garcia-Mateo, C. Capdevila, F. G. Caballero, C. G. DeAndres: ISIJ Int., 48 (9) (2008)1270-1275.

[20] G. I. Rees and H.K. D. H. Bhadeshia: Mat. Sci. and Tech.,10 (1994) 353.

[21] S.S. Babu and H.K.D.H. Bhadeshia: Mat. Sci. and Tech., 6 (1990) 1005-1020.

[22] I. Madariaga, I . Gutierrez, C. G. Deandres and C. Capdevila: Scripta Mater., 41 (1999) 229.

[23] I. Madariaga, I. Gutierrez, H.K.D.H. Bhadeshia: Metall. Trans., A 32A (9) (2001) 2187-2197.

[24] T. Furuhara, T. Shinyoshi, G. Miyamoto, J. Yamaguchl, N. Sugita, N. Kimura, N. Takemura and T. Maki: ISIJ Int., 43 (12) (2003) 2028-2037.

[25] C. G. De Andres, C. Capdevila, D. San Martin and F. G. Caballero : J. of Mat. Sci., 20 (2001) 1135 –1137.

[26] C. Garcia de Andres, F.G. Caballero, C. Capdevila, D. San Martin : Mater. Charact., 49 (2003) 121-127.

[27] C. Garcia de Andres, M.J. Bartolome, C. Capdevila, D. San Martin, F.G. Caballero and V. Lopez: Mater Charact., 46 (2001) 389-398.

[28] H. Adrian: Proc. of Int. Conf. Microalloying ’95, ISS, Warrendale,PA, USA,1995, p. 285.

[29] C. Capdevila, F. G. Caballero. C. Gracia-Mateo and C. Garcia de Andres: Mater. Trans., 45 (2004), 2678.

[30] C. Capdevila, F. G. Caballero, and C. Garcia de Andres: Mater. Sci. Technol., 19 (2003) 195-201.

[31] C. Capdevila, F.G. Caballero, and C. Garcia de Andres: Met. and Mat. Trans.A., 32A (2001) 1591-1597.

[32] M. Dıaz-Fuentes, I. Gutiérrez: Mat. Sci and Eng., A363 (2003) 316-324.

[33] H. K. D. H. Bhadeshia and D.V.Edmonds: Metall. Trans., A10 (1979) 895-907.

[34] T. Ochi, T. Takahashi and H. Takada: Mechanical Working and Steel Processing Conf. Proe. , ISS-AIME, Warrendale, PA,USA, 1988, p. 65-72.

[35] F. Ishikawa, T. Takahashi, T. Ochi: Metall. Mater. Trans., 25A (5) (1994) 929-936..

[36] S. Zajac: Mat. Sci. Forum., 500-501(2005) 75-86.

[37] M.J. Balart, C.L. Davis, M. Strangwood: Mat. Sci. And

Eng., A328 (2002) 48-57.

[38] Z. Zhao, et al: Journal of Materials Science., 36 (2001) 5045-5056.

[39] H.K.D.H. Bhadeshia and R.W.K.Honeycombe: Steels Microstructure and Properties, Elsevier Ltd, London 2006, p.147.

[40] Y. K. Lee: J. of Mat. Sci. Letters., 21(2002) 1253-1255.

[41] Antonio Augusto Gorni: Steel Forming and Heat Treating Handbook, São Vicente, Brazil 2011, p.24.

[42] J. Wang, P. van der Wolk and S. van der Zwaag: Mater. Trans., JIM, 41(7) (2000) 761-768.

[43] B. Mintz, The influence of aluminium on the strength and impact properties of steel, Int. Con. on TRIP-aided H. S. Ferrous Alloys, Ghent, Belgium, 2002, p. 379-382

[44] S. Chupatanakul, P. Nash, and D. Chen: Met. and Mat. Int.,12 (2006) 453-458.

[45] M. Arjomandi, H. Khorsand, S. H. Sadati and H. Addoos: Defect and Diffusion Forum., 273-276 (2008) 329-334.